Electrodeposition of a palladium nanocatalyst by ion confinement in polyelectrolyte multilayers†

Miguel Vago,[a] Mario Tagliazucchi,[a] Federico J. Williams[ab] and Ernesto J. Calvo*[a]

Received (in Cambridge, UK) 16th July 2008, Accepted 3rd September 2008
First published as an Advance Article on the web 3rd October 2008
DOI: 10.1039/b812181h

A highly efficient and selective material for electrocatalytic hydrogenation has been prepared by depositing monodisperse palladium nanoparticles of size (6±1) nm by electrochemical reduction of $PdCl_4^{2-}$ confined in a polyelectrolyte multilayer film.

Electrochemical deposition is an attractive route to modify conductive substrates with functional metallic nanostructures.[1–6] Electrodeposition of small monodisperse nanoparticles requires limiting diffusion of metal ions towards the electrode in order to control crystal nucleation and growth. Several strategies have been proposed to achieve this goal, such as using a template,[4] applying very short electrodeposition pulses[1–3,6] or slowing down ion diffusion by increasing the solution viscosity.[2] Supported Pd nanocatalysts are important due to their technological applications in fuel cells, electrosynthesis and electrochemical sensors. In the present work, we disclose a new method to electrodeposit Pd nanoparticles from metal ions confined in a polyelectrolyte multilayer film (PEM) electrostatically self-assembled on carbon felt electrodes. The resulting electrocatalyst presents a higher catalytic efficiency per mole of metal catalyst and a higher product selectivity than electrodes modified by direct electroreduction of Pd ions, which are routinely used in electrocatalytic hydrogenation.[7–9]

Rubner, Cohen and co-workers were the first to describe a method that uses PEMs as nanoreactors to grow inorganic nanocrystals from coordinated metal ions:[10–12] electrostatically self-assembled multilayers were immersed in a solution of the cations (Ag^+, Pb^{2+} or $Pd(NH)_4^{2+}$), which bind to carboxylic groups in poly(acrylic acid) (PAA). The ion exchanged cations incorporated in the film were subsequently converted into nanoparticles through a chemical reaction (*i.e.* reduction or sulfidation). Bruening *et al.* developed an alternative method where palladium ions were co-deposited during multilayer formation.[13,14] Highly size-selective[14] hydrogenation of unsaturated alcohols has been achieved by alumina colloids modified in this way. Palladium nanoparticles were also obtained in multilayer films built by alternate adsorption of $PdCl_4^{2-}$ and electro-deposition of osmium redox polymer, *i.e.* quaternized poly(vinylpyridine), QPVP-Os.[16] Electroreduction of adsorbed Pd^{2+} has been employed to decorate multiwall carbon nanotubes with sub-nanoparticles.[15]

In the present Communication we report the ion exchange of $PdCl_4^{2-}$ in a multilayer comprised of self assembled poly(allylamine) (PAH) and poly(acrylic) acid (PAA) to yield highly selective nanocatalysts.

Unlike previous work, nanoparticles have been produced on the carbon surfaces by electrochemical rather than chemical reduction, with the advantage of avoiding the use of strong, soluble reducing agents[14] (which therefore eliminates the problem of waste disposal or the manipulation of hydrogen gas[10]).

Fig. 1A shows an SEM image of carbon felt fibers modified with a (PAH/PAA)PAH PEM with 2 ion exchange/ reduction cycles, hereafter denoted (PAH/PAA)PAH + 2Pd following the nomenclature introduced by Rubner and co-workers.[11] Fig. 1A shows no evidence of micrometer sized particles. A

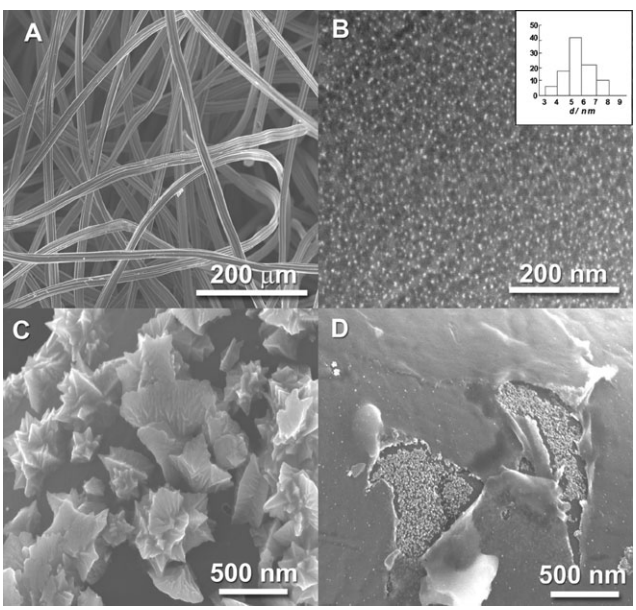

Fig. 1 Scanning electron micrograph (SEM) of modified carbon felt electrodes: (A) (PAH/PAA)PAH + 2Pd (low magnification). (B) (PAH/PAA)PAH + 2Pd (high magnification). (C) Electrode modified by direct electroreduction of $PdCl_4^{2-}$ at 300 mV for 180 s. (D) (PAH_4/PAA_4)PAH + 4Pd. Note that in sample (D), Pd nanoparticles are only visible in delaminated zones. Overlay in (B): histogram of Pd nanoparticle diameters.

[a] *INQUIMAE, Departamento de Química Inorgánica, Analítica y Química Física Facultad de Ciencias Exactas y Naturales, Universidad de Buenos Aires, Buenos Aires, C1428EHA, Argentina*
[b] *Department of Surface Chemistry and Coatings, Center for Industrial Research, TENARIS, Dr Simini 250, Buenos Aires, B2804MHA, Campana, Argentina*

† Electronic supplementary information (ESI) available: Details of experimental methods, XPS spectra in the Pd 3d region and ellipsometric thickness *vs.* number of layers for the PAH/PAA system on HOPG. See DOI: 10.1039/b812181h

magnified image of a carbon fiber (Fig. 1B) reveals the presence of homogeneously distributed (6 ± 1) nm nanoparticles (this size may actually be an upper limit since smaller particles would be below the SEM resolution, but could still be detected by electrochemical experiments). As a control experiment, Pd nanoparticles were absent in a bare carbon felt electrode exposed to an ion exchange/reduction cycle. Micro-sized crystals prepared by direct electroreduction of $PdCl_4^{2-}$ solution are shown in Fig. 1C for comparison.

We have studied nanoparticle formation as a function of the thickness of the confined ion layer, determined by the number of polyelectrolyte adsorption steps (see ellipsometric data in Fig. 2S, ESI†).

Thin films (Fig. 1B) exhibit a homogeneous distribution of Pd nanoparticles, while non-homogeneous distribution is observed in thick films $(PAH_4/PAA_4)PAH$ + 4Pd (Fig. 1D). In the latter case two regions are observed: a continuous film without nanoparticles on the surface and delaminated regions (probably caused by mechanical stress due to hydrogen evolution) with homogeneous particle distribution. Therefore nanoparticles are preferentially located at the electrode/film interface. Unlike chemical reducing agents,[11,12,14] which can homogenously access the entire PEM, electron transfer from the underlying electrode to ions entrapped in the film is limited to tunneling distance ($d < 10$ Å) and Pd(II) ions coordinated in the film must approach the electrode in order to be reduced.

We have also examined the fraction of reduced Pd by following the XPS Pd 3d peak (see Fig. 1S, ESI†). The thinnest possible film, PAH + 2Pd, showed 80% Pd^0, which is a similar fraction to that reported for chemically reduced cations confined in self-assembled multilayers.[14] We expect XPS to probe the whole PAH layer, since its thickness (1.5 nm) is smaller than the photoelectron inelastic mean free path in the film (~3 nm[17]). On the other hand, only 22% Pd^0 was measured for the thickest films studied, $(PAH_4/PAA_4)PAH$ + 2Pd. Since the thickness in the latter case is 43 nm, XPS can only probe the region closest to the upper film surface. These results confirm that Pd nanoparticles have been electrodeposited at the film/electrode interface while a fraction of Pd(II) ions far from the electrode remain immobilized within the film. Since metal ions far from the film/electrode interface remain unreduced, an efficient use of Pd would require a fine adjustment of the PEM thickness, which can be achieved by designing the number of polyelectrolyte layers.

Electrochemically deposited palladium nanoparticles are in electrical contact with the electrode and thus electrochemically active. This is confirmed by the characteristic cyclic voltammetry in the oxide and hydrogen evolution regions, which are depicted in Fig. 2A and B, respectively (solid lines). In addition, current–potential curves for an electrode obtained by direct electroreduction of $PdCl_4^{2-}$ ions (large crystals in Fig. 1C) are shown for comparison. While both electrodes present qualitatively all the features expected for a bulk Pd, Fig. 2A shows that the potential of the palladium oxide reduction peak for the nanoparticle modified electrode (482 mV *vs.* NHE) is negatively shifted with respect to the large particle Pd modified electrode (595 mV) and to the potential reported for bulk Pd (600–800 mV).[18] A small negative shift of the PdO reduction peak with decreasing

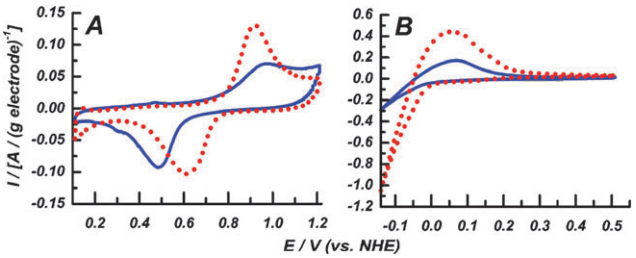

Fig. 2 Cyclic voltammograms (normalized by the mass of the electrode) for a $(PAH_2/PAA_2)PAH$ + 2Pd nanoparticle modified electrode (solid blue lines) and a microparticle modified electrode (red dashed lines) obtained from direct electrodeposition from aqueous $PdCl_4^{2-}$ solution at 300 mV for 180 s. The Pd oxide (A) and hydrogen adsorption (B) regions are presented separately.

particle size has been reported for electrodes modified by impregnation and reduction of Pd salts.[19] From the integrated charge of the PdO reduction peak it is possible to estimate the electrochemical active area of the Pd deposition.

Similar electroactive Pd areas per gram of carbon fiber have been determined by integration of the oxide reduction peak in Fig. 2. However, the percentage of Pd mass relative to carbon fiber mass, determined by ICP is almost ten times lower for the nanoparticles (0.0800 ± 0.0005%), than for the microparticles (0.7 ± 0.1%). Therefore, a much higher surface to volume ratio is achieved for the nanoparticle deposition since the specific areas normalized per gram of Pd catalyst are respectiverly 82 $m^2\ g^{-1}$ and 10 $m^2\ g^{-1}$ for the nano and microparticle electrodes. Moreover, the real value for the nanoparticle electrode would be somewhat higher, since XPS shows that only a fraction of the Pd atoms on the film surface are reduced. It is also interesting to highlight the agreement between the specific area for this electrode with the expected area for hemi-spherical 6 nm Pd particles (83 $m^2\ g^{-1}$).

Fig. 2B shows that during the cathodic scan both hydrogen adsorption and absorption occur followed by hydrogen evolution at $E < 0.0$ V. The stripping of adsorbed and dissolved hydrogen in the metal occurs during the oxidative scan, separated by some tens of millivolts.[19] In our hands, both processes appear overlapped producing a single peak. It should be noted that in spite of the similar electroactive areas for both electrodes compared in Fig. 2B, the microparticle electrode presents a hydrogen stripping charge that is twice that for the nanoparticle electrode. We attribute this difference to a larger amount of dissolved hydrogen in the micro-crystalline sample due to its larger Pd content.

Electrocatalytic hydrogenation is an interesting alternative to traditional heterogeneous catalytic hydrogenation which allows the reduction of unsaturated organic species without the risks of using and handling H_2 gas. The electrocatalytic properties of nanoparticles $(PAH_2/PAA_2)PAH$ + 2Pd) and microparticles have been studied with the model hydrogenation reaction of acetophenone in acidic hydro-alcoholic solution.[8,9]

The process was carried out in a two-compartment batch reactor monitoring the acetophenone $n \rightarrow \pi^*$ absorption band at 285 nm, which is absent in the reaction products. Fig. 3 depicts the acetophenone concentration decay for both

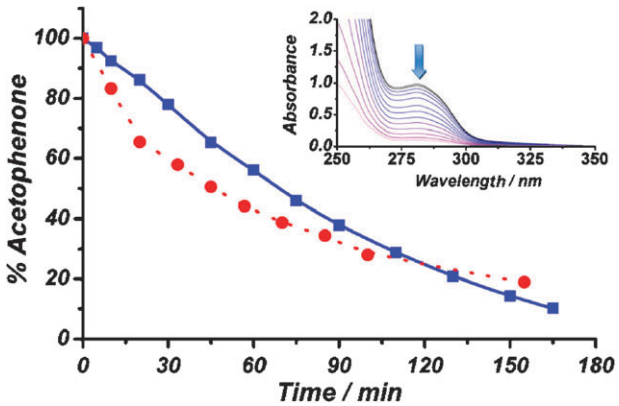

Fig. 3 Concentration of acetophenone determined by UV spectroscopy as a function of electroreduction time for a batch process at −500 mV in an acidic hydro-alcoholic solution using a $(PAH_2/PAA_2)PAH + 2$ Pd nanoparticle modified electrode (blue line) or a microparticle electrode generated by direct electroreduction of aqueous $PdCl_4^{2-}$ (red dashed line). The palladium electrochemically active areas were 28 cm^2 and 33 cm^2, respectively. Inset: time evolution of solution spectra showing the disappearance of the acetophenone band at 285 nm for the nanoparticle modified electrode.

electrodes which is similar and consistent with the fact that both catalysts have comparable electrochemically active areas. Since the Pd content of the nanoparticle modified electrode is a tenth of that for the microparticle one, the efficiency per gram of noble metal catalyst is much higher for the former. In other words, the improvement in electrocatalytic efficiency is a consequence of the larger Pd area to volume ratio for the nanoparticle electrodes. In addition, HPLC analysis of reaction products shows that the nanoparticle modified electrode exhibits a 100% selectivity towards the formation of phenyl ethanol at 90% conversion. This result is noteworthy since we found 84% selectivity (16% of ethylbenzene as a secondary product) for the microparticle electrode at a similar conversion, in agreement with literature reports[8] which show that ethylbenzene is always obtained in a proportion from 15% to 50%. It has been suggested in the literature[8] that ethylbenzene and phenyl ethanol are formed through parallel pathways on different active sites on the catalyst surface, and therefore their final ratio would depend on the proportion of each site, which in turn would depend on the size of the catalyst crystals. We should point out that both the catalytic activity and the electrochemical surface area remains unmodified after 120 min of continuous operation.

Our results demonstrate that homogeneous metal nanoparticles can be electrodeposited within polyelectrolyte multi-layers resulting in electrodes with enhanced performance as compared to electrodes containing microparticles. The improvement is both in efficiency (due to the large area to volume ratio) and product selectivity.

We expect to extend this method to other noble metal electrocatalysts, including bimetallic ones and, by virtue of the layer by layer self-assembly to apply them to substrates of any shape and size.

Notes and references

1 J.-C. Bradley, S. Babu, A. Mittal, P. Ndungu, B. Carroll and B. Samuel, *J. Electrochem. Soc.*, 2001, **148**, C647–C651.
2 X. Chen, N. Li, K. Eckhard, L. Stoica, W. Xia, J. Assmann, M. Muhler and W. Schuhmann, *Electrochem. Commun.*, 2007, **9**, 1348–1354.
3 M. O. Finot, G. D. Braybrook and M. T. McDermott, *J. Electroanal. Chem.*, 1999, **466**, 234–241.
4 K. Nielsch, F. Müller, A.-P. Li and U. Gösele, *Adv. Mater.*, 2000, **12**, 582.
5 R. M. Penner, *J. Phys. Chem. B*, 2002, **106**, 3339–3353.
6 J. V. Zoval, J. Lee, S. Gorer and R. M. Penner, *J. Phys. Chem. B*, 1998, **102**, 1166–1175.
7 M. Vago, F. J. Williams and E. J. Calvo, *Electrochem. Commun.*, 2007, **9**, 2725–2728.
8 A. M. Polcaro, S. Palmas and S. Dernini, *Ind. Eng. Chem. Res.*, 1993, **32**, 1315–1322.
9 A. M. Polcaro, S. Palmas and S. Dernini, *Electrochim. Acta*, 1993, **38**, 199–203.
10 S. Joly, R. Kane, L. Radzilowski, T. Wang, A. Wu, R. E. Cohen, E. L. Thomas and M. F. Rubner, *Langmuir*, 2000, **16**, 1354–1359.
11 T. C. Wang, M. F. Rubner and R. E. Cohen, *Langmuir*, 2002, **18**, 3370–3375.
12 T. C. Wang, M. F. Rubner and R. E. Cohen, *Chem. Mater.*, 2003, **15**, 299–304.
13 J. Dai and M. L. Bruening, *Nano Lett.*, 2002, **2**, 497–501.
14 S. Kidambi and M. L. Bruening, *Chem. Mater.*, 2005, **17**, 301–307; S. Kidambi, J. Dai, J. Li and M. L. Bruening, *J. Am. Chem. Soc.*, 2004, **126**, 2658–2659.
15 X. Ji, C. E. Banks, A. F. Holloway, K. Jurkschat, C. A. Thorogood, G. G. Wildgoose and R. G. Compton, *Electroanalysis*, 2006, **18**, 2481–2485.
16 J. Liu, L. Cheng, Y. Song, B. Liu and S. Dong, *Langmuir*, 2001, **17**, 6747–6750.
17 M. Tagliazucchi, F. Williams and E. J. Calvo, *J. Phys. Chem. B*, 2007, **111**, 8105–8113.
18 C. Gabrielli, P. P. Grand, A. Lasia and H. Perrot, *J. Electroanal. Chem.*, 2004, **151**, A1937.
19 R. Pattabiraman, *Appl. Catal., A*, 1997, **153**, 9–20.